

***mnd2*: A New Mouse Model of Inherited Motor Neuron Disease**

JULIE M. JONES,* ROGER L. ALBIN,† EVA L. FELDMAN,† KARL SIMIN,*
TIMOTHY G. SCHUSTER,* WESLEY A. DUNNICK,‡ JOHN T. COLLINS,‡
C. E. CHRISP,§ BENJAMIN A. TAYLOR,|| AND MIRIAM H. MEISLER*¹

Departments of *Human Genetics, †Neurology, ‡Microbiology and Immunology, and §Laboratory Animal Medicine, University of Michigan Medical School, Ann Arbor, Michigan 48109; and ||The Jackson Laboratory, Bar Harbor, Maine 04609

Received December 15, 1992; revised February 19, 1993

The autosomal recessive mutation *mnd2* results in early onset motor neuron disease with rapidly progressive paralysis, severe muscle wasting, regression of thymus and spleen, and death before 40 days of age. *mnd2* has been mapped to mouse chromosome 6 with the gene order: *centromere-Terb-Ly-2-Sftp-3-D6Mit4-mnd2-D6Mit6, D6Mit9-D6Rck132-Raf-1, D6Mit11-D6Mit12-D6Mit14*. *mnd2* is located within a conserved linkage group with homologs on human chromosome 2p12-p13. Spinal motor neurons of homozygous affected animals are swollen and stain weakly, and electromyography revealed spontaneous activity characteristic of muscle denervation. Myelin staining was normal throughout the neuraxis. The clinical observations are consistent with a primary abnormality of lower motor neuron function. This new animal model will be of value for identification of a genetic defect responsible for motor neuron disease and for evaluation of new therapies. © 1993 Academic Press, Inc.

INTRODUCTION

Human motor neuron disease is a common and untreatable neurologic syndrome characterized by degeneration of spinal and bulbar motoneurons (lower motor neurons), often accompanied by degeneration of corticospinal and corticobulbar neurons (upper motor neurons). The muscular weakness caused by motor neuron disease is progressive and death usually ensues within a few years of diagnosis. While most cases are sporadic, approximately 5-10% of all cases have a family history (Brooke, 1986). Differing patterns of inheritance and age of onset among pedigrees suggest the existence of considerable genetic heterogeneity. Within the past 2 years there has been dramatic progress in genetic mapping of some of the responsible genes: spinal motor atrophy (SMA) on chromosome 5q13 (Brzustowicz *et al.*, 1990; Melki *et al.*, 1990); amyotrophic lateral sclerosis 1

(*ALS1*) on chromosome 21q22 (Siddique *et al.*, 1991), and amyotrophic lateral sclerosis 2 (*ALS2*) on chromosome 2q31-q35 (Hentati *et al.*, 1992). Work is in progress in several laboratories to isolate these genes by positional cloning.

Genetic mutations in other species can provide important models for identification of the underlying defects and development of therapy. In view of the genetic heterogeneity of the human disease, it will be useful to analyze a variety of mutants to gain a better understanding of the pathogenesis of motoneuron degeneration. In this report we describe a new mouse model of inherited motor neuron disease.

MATERIALS AND METHODS

Animals. Inbred mice of strains C57BL/6J, CAST/Ei, CASA/Rk, and MEV were obtained from the Jackson Laboratory (Bar Harbor, ME). *wst/+* mice were provided by Dr. Leonard Shultz, The Jackson Laboratory. Transgenic founder 283 was generated by microinjection of CAT construct 5 into fertilized eggs of (C57BL/6J × C3H/He)F₂ mice (Keller *et al.*, 1990). Line 283 was generated by crossing the founder with inbred strain C57BL/6J and maintained by continued crossing with C57BL/6J. *mnd2/+* heterozygous carriers in each generation were identified by test crossing with known heterozygotes and identification of affected offspring. These experiments were approved by the University of Michigan Committee on Use and Care of Animals and animals were housed and cared for according to NIH guidelines.

Linkage analysis. Genomic DNA was isolated from brain by RNase and proteinase K treatment followed by phenol/chloroform extraction and ethanol precipitation. Polymerase chain reaction for *Terb* (Hearne *et al.*, 1991) and the *Mit* markers (Dietrich *et al.*, 1992) was carried out as described except that 100 ng of template DNA was used and products were labeled by incorporation of [α -³²P]dCTP (>3000 Ci/mmol, Amersham) (1 μ Ci per 10- μ l reaction) with a 40-fold reduction of unlabeled dCTP. Three loci were typed by Southern blotting. To identify restriction fragment length variation, genomic DNA was digested with a variety of restriction endonucleases and hybridized with the appropriate probes. We identified a *castaneus*-specific 2.9-kb *TaqI* fragment at the *Raf-1* locus (Kozak *et al.*, 1984), a 1.4-kb *Sau3A* fragment at the *D6Rck132* locus (Bahary *et al.*, 1991), and *BglII* fragments of 3.6, 4.4, and 12.1 kb at the *Sftp-3* locus (Moore *et al.*, 1992).

Histology. Mice were deeply anesthetized with ketamine/xylazine and transcardially perfused with 5 ml of 0.1 M phosphate-buffered saline, pH 7.4, followed by 10 ml of 4% paraformaldehyde, 0.1 M phosphate buffer, pH 7.4 (PB). The brain and spinal cord were removed and immersed in fixative overnight at 4°C, transferred to 20% su-

¹ To whom correspondence should be addressed at Department of Human Genetics, 4708 Medical Sciences 2, Ann Arbor, MI 48109-0618. Telephone: (313) 763 5546. Fax: (313) 763 3784.

crose-PB containing 0.02% sodium azide, and stored at 4°C. Forty-micrometer frozen sections were cut on a sliding microtome and collected in PB containing 0.02% sodium azide. For routine histology, sections were stained with 0.5% cresyl violet or for myelin as described previously (Kaatz *et al.*, 1992). Phosphorylated neurofilaments were identified with 1/2000 diluted monoclonal antibody SMI-31 (Sternberger-Meyer, Jarrettsville, MD). Immunoreactivity was visualized with the avidin-biotin conjugate method using a Vectastain kit (Vector, Burlingame, CA). The presence of astrogliosis was evaluated by glial fibrillary acidic protein immunohistochemistry (primary antibody, Dako 1/500) using an indirect peroxidase technique (McKeever and Balentine, 1987).

The entire neuraxis with the exception of thoracic spinal cord was sectioned from three *mnd2/mnd2* affected animals and six series of sections were collected. Severely affected animals between 34 and 38 days of age were analyzed. One series from each animal was stained with cresyl violet and a second series was stained for myelin. For immunohistochemistry, the spinal cords of five *mnd2/mnd2* affected individuals and three unaffected littermates were examined.

For electron microscopic examination, two *mnd2/mnd2* mice and two control littermates were anesthetized and perfused as described above with 2% glutaraldehyde in 0.05 M sodium cacodylate buffer. Brain and spinal cord were postfixed in the same fixative at 4°C, and 2-mm blocks of spinal cord were embedded in Polybed (Polysciences). Silver-gold sections were stained on copper grids with uranyl acetate and lead citrate. Grids were viewed on a JEOL 100S electron microscope.

Thymus and spleen were fixed in 10% buffered formalin, embedded in paraffin, and stained with hematoxylin and eosin.

Nerve and muscle function. Mice between the ages of 30 and 32 days were anesthetized with ketamine/xylazine. Motor nerve conduction were recorded as described by Parry and Koza (1990). Compound muscle action potentials were recorded from the gastrocnemius after stimulation of the sciatic-tibial nerves, and distal motor latencies and conduction velocities were calculated. Needle electromyography was performed on selected hind limb and lumbar paraspinal muscles. Three limbs were examined on each of eight affected animals.

Immunology. Immunoglobulin isotype expression in serum was determined by ELISA using alkaline phosphatase-conjugated goat antibodies specific for mouse IgM, IgG1, IgG2a, IgG2b, IgG3, IgA, and kappa light chains (Southern Biotechnology Associates and Boehringer-Mannheim). Lymphoid cell surface marker expression was determined using an EPICS C flow cytometer. Thymocytes or total splenocytes were stained on ice with rat anti-mouse Thy-1.2, hamster anti-mouse CD3 ϵ , or biotinylated goat anti-mouse Lyt 1, Lyt 2, or IgM.

RESULTS

Origin of the *mnd2* Mutation

Mice with a severe wasting disease were observed among the progeny of heterozygous transgenic mice descended from founder 283 microinjected with a 2-kb transgene (Keller *et al.*, 1990). The transgene insertion site was cloned from genomic DNA and used to probe Southern blots. The probe hybridized with a 14-kb *Bgl*II fragment in nontransgenic DNA and a 16-kb *Bgl*II fragment in homozygous transgenic DNA. Obligate heterozygotes contain both the 14- and the 16-kb bands. The genotypes of affected animals included both types of homozygotes as well as heterozygotes, demonstrating that disease status is unrelated to transgene status. Homozygous nontransgenic, affected mice did not contain any transgene sequences detectable by Southern blotting with the transgene probe.

It seems most likely that the *mnd2* mutation was caused by the microinjection procedure. For example, deletion of a second site insert in founder 283 could account for the observations. Alternatively, *mnd2* may have arisen as a spontaneous mutation fortuitously carried by the founder animal.

Time Course of the Wasting Disease in Affected Animals

Affected animals can be recognized between 21 and 24 days of age by their unsteady gait with extended hind limbs, as if they are walking on tiptoe. Continued atrophy of the hind leg muscle results in a characteristic hunched posture, loss of balance, and difficulty in recovering from a reclining position. During disease progression, the animals fail to gain weight and their growth falls significantly behind that of their unaffected littermates (Fig. 1). There is progressive decline in mobility and the animals die within 2 weeks of onset, usually prior to 40 days of age. Intra-gastric feeding did not delay the onset or progression of symptoms.

Mode of Inheritance

One hundred and fifty-eight affected animals have been obtained from crosses between unaffected carriers

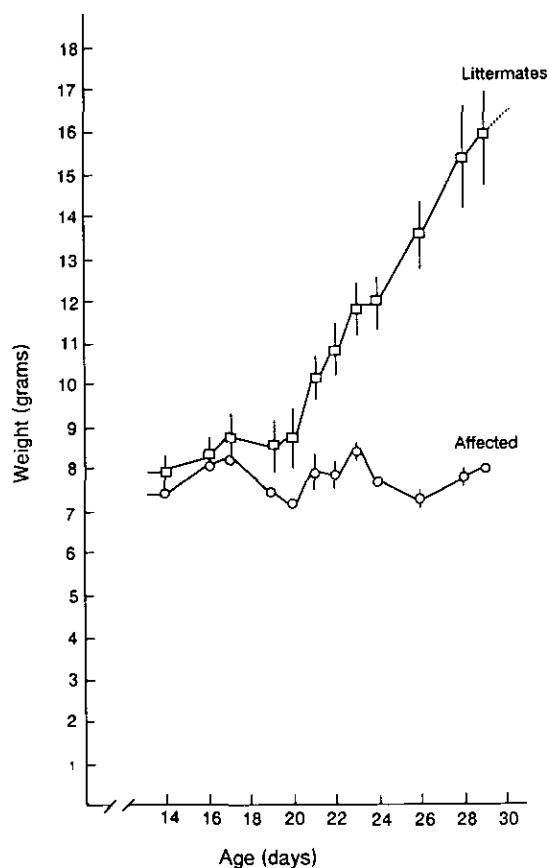


FIG. 1. Growth retardation in affected mice. Eleven individuals from one litter were weighed daily. Symbols represent means and vertical lines indicate standard deviations of values for three affected individuals and eight unaffected littermates.

TABLE 1
Autosomal Recessive Inheritance
of Motor Neuron Disease

Cross	Offspring			
	Affected	Unaffected	Total	% Affected
283 × 283	95	384	479	20
(283 × CASA)F ₁ × 283	8	34	42	19
(283 × CAST)F ₂	26	80	106	25
(283 × MEV)F ₂	29	84	113	26
Total:	158	582	740	21

Note. All parental animals in the crosses were heterozygous carriers of the *mnd2* allele. The numbers of affected and unaffected offspring of each cross are indicated. Line 283-*mnd2* was generated from the transgenic founder and maintained by continuous crossing with C57BL/6J. CASA/Rk (CASA) and CAST/Ei (CAST) are inbred strains derived from the subspecies *M. m. castaneus*. Strain MEV is derived from C58/J and the AKXD-14 recombinant inbred strain (Taylor and Rowe, 1989).

on several genetic backgrounds (Table 1). The observation of 21% affected offspring is consistent with autosomal recessive inheritance with complete penetrance ($\chi^2 = 2.1, P > 0.1$). The recessive mutation responsible for the inherited disorder has been designated *motor neuron degeneration-2*, with the gene symbol *mnd2*.

Genetic Mapping of the mnd2 Locus

mnd+/+ heterozygotes from line 283 were crossed with the MEV linkage testing stock, which is marked with

several unlinked endogenous viruses (Taylor and Rowe, 1989). F₁ mice were crossed and affected F₂ offspring were analyzed. Genomic DNA from 16 affected and 1 unaffected individual was tested by Southern blotting with an ecotropic-specific mouse leukemia virus probe. All of the endogenous retroviral loci segregated independently of the *mnd2* locus, allowing the exclusion of linkage from large portions of chromosomes 1-5, 7-9, 11, 18, and 19.

To test the rest of the genome, *mnd2*/+ heterozygotes from line 283 were crossed with inbred *castaneus* strains CAST/Ei and CASA/Rk. Heterozygous CASA/Rk F₁ offspring were identified by test crossing with *mnd*+/+ heterozygotes from line 283; eight affected offspring were obtained from this mating. Intercrosses between randomly paired CAST/Ei F₁ animals generated 23 affected F₂ mice. Genomic DNA from affected mice was tested for linkage with microsatellite markers containing (CA)_n repeats (Dietrich *et al.*, 1992). Linkage was observed with microsatellite markers on chromosome 6. Further localization was obtained by analysis of the well-mapped genes *Raf-1*, *Sftp-3*, and *Ly-2* (D6Mit16) (Elliott and Moore, 1992). The results of the linkage analysis are presented in Fig. 2. The data indicate that *mnd2* is located in the interval between D6Mit4 and D6Mit6 in the central region of chromosome 6.

Morphology of Spinal Motor Neurons

Cresyl violet staining of affected *mnd2* mice revealed normal cytoarchitecture and neuronal morphology in

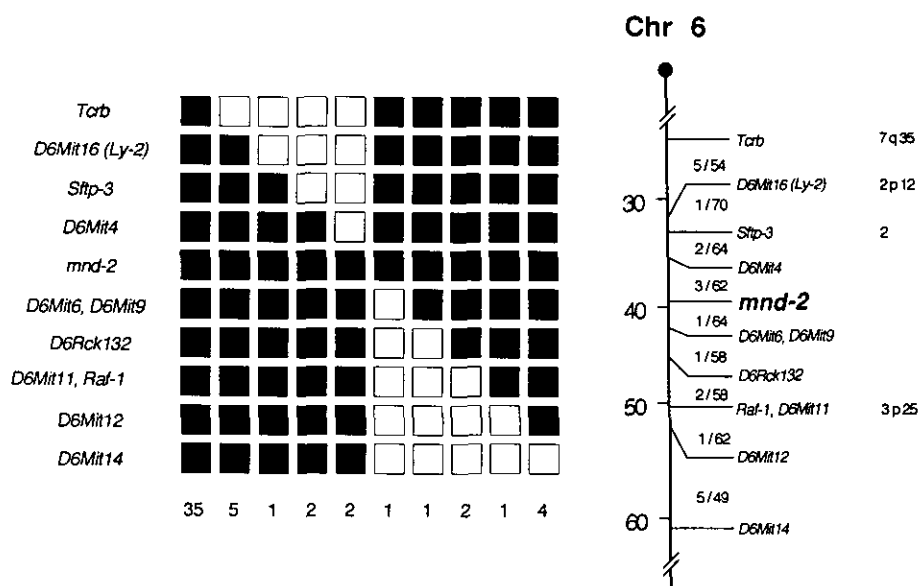


FIG. 2. Chromosome location and haplotype data for the *mnd2* locus on mouse Chromosome 6. Heterozygous *mnd2*/+ mice from line 283 were crossed with strain CAST/Ei. Genomic DNA was obtained from 23 affected F₂ intercross mice and 8 affected backcross animals. All of the analyzed individuals carry two *mnd2* mutant alleles. Each column contains the haplotype of recombinant chromosomes that were observed, and the number of mice with each haplotype is given at the bottom of each column. Haplotypes of F₂ progeny were inferred by assuming the absence of double crossovers between markers in this 29-cM region. The approximate map positions are given in cM from the centromere (Elliott and Moore, 1992). The fraction of recombinant animals observed for each interval is shown to the right of the chromosome map; some of these animals are not included in the haplotype table. The positions of the human homologs are indicated at the far right. Solid boxes, C57BL/6J homozygotes; open boxes, heterozygotes with C57BL/6J and CAST/Ei alleles.

the forebrain, cerebellum, and brainstem. Myelin staining was normal throughout the neuraxis (Fig. 3). In the spinal cord, the degree of cellularity appeared normal. Most spinal neurons had normal morphology, except that the motoneurons had a swollen, spherical appearance and weak staining intensity (Fig. 4C). The abnormal morphology of these motor neurons is similar to that seen in human motor neuron disease (Brooke, 1986). Abnormal motoneurons were observed consistently in multiple affected animals. In contrast, unaffected littermates contained numerous darkly stained motoneurons with characteristic polygonal appearance

(Fig. 4A). Swollen motoneurons were observed in both cervical and lumbar regions of the spinal cords of affected mice. The appearance of dorsal horn cells was normal. There was no increase in glial fibrillary acidic protein immunoreactivity in the ventral horn, indicating lack of reactive gliosis (not shown).

Electron microscopic examination revealed chromatolytic neurons with loss of rough endoplasmic reticulum and abnormal folding of the nuclear membrane. There were no inclusions, vacuoles, or aggregations of neurofilaments, indicating that *mnd2* does not produce a storage disease (unpublished observations).

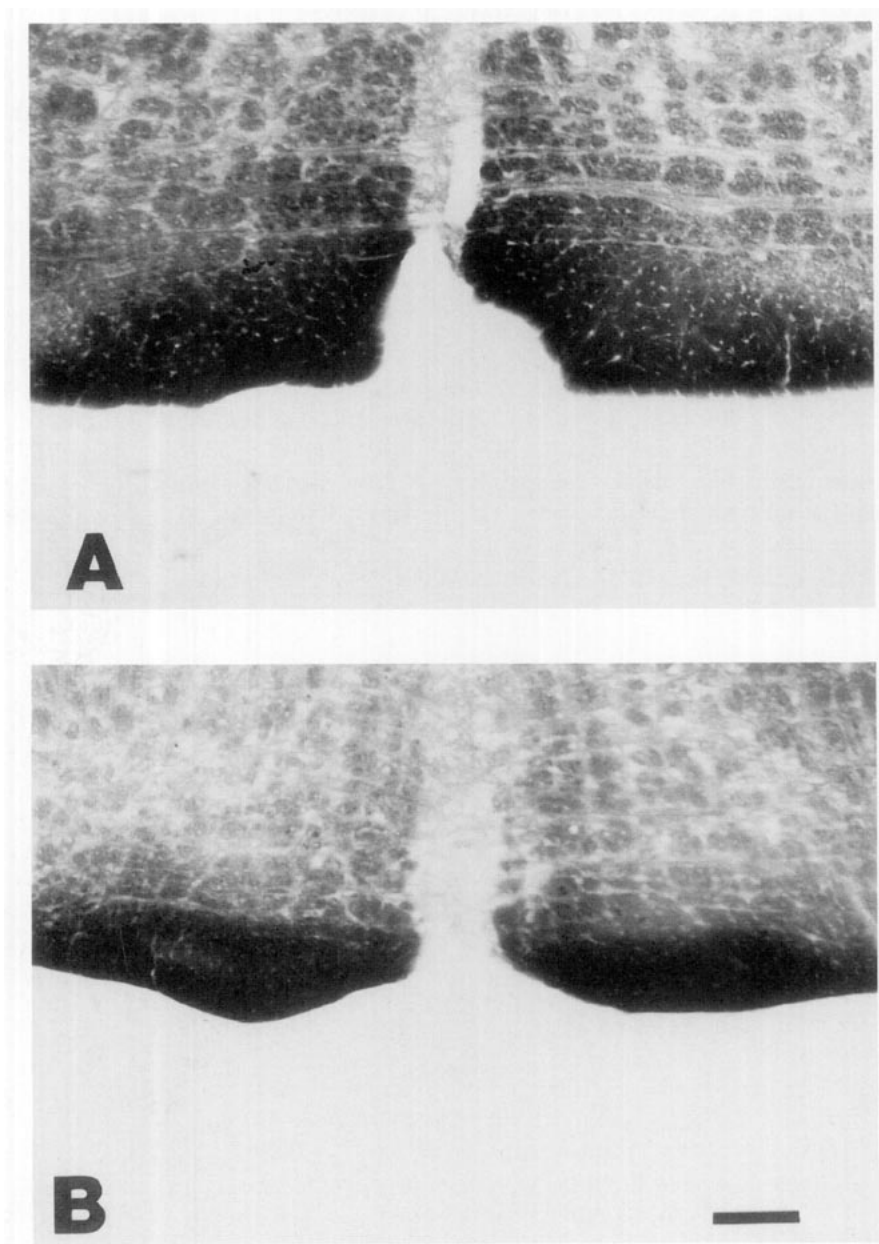


FIG. 3. Myelin staining in the corticospinal tract. Brains were sectioned at the level of the rostral medulla to demonstrate the corticospinal tract on the ventral surface of the brain stem. Myelin was stained as described (Kaatz *et al.*, 1992). (A) control; (B) *mnd2/mnd2* affected animal. Scale bar = 1 mm.

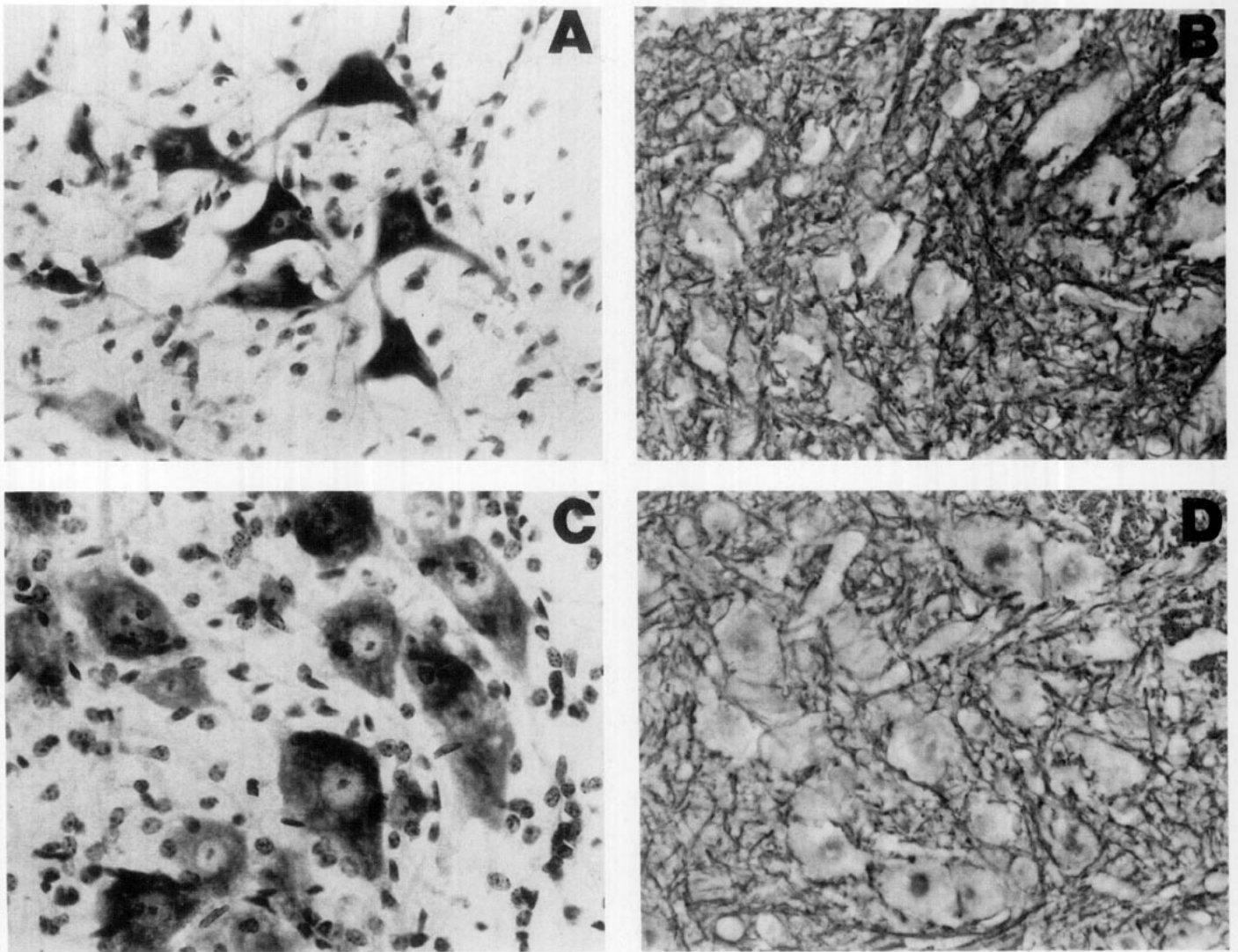


FIG. 4. Morphology of spinal motor neurons. Sections at the level of the cervical spinal cord were stained with cresyl violet (left) or with a monoclonal antibody to phosphorylated neurofilaments (right). Control mice have darkly stained polygonal perikarya (A) and lack phosphorylated neurofilaments within the perikarya (B). *mnd2/mnd2* mice have lighter staining, swollen perikarya with loss of normal polygonal morphology (C). *mnd2/mnd2* mice do not contain phosphorylated neurofilament immunoreactivity within the perikarya (D). (A, B) Normal; (C, D) *mnd2/mnd2*. Scale: 1.7 cm = 50 μ m.

Normal Distribution of Phosphorylated Neurofilaments in *mnd2/mnd2* Mice

The monoclonal antibody SMI-31 identifies predominantly the phosphorylated form of heavy (200 kDa) neurofilaments (Sternberger and Sternberger, 1983). SMI-31 immunoreactivity was restricted to axons in control animals (Fig. 4B) and in affected *mnd2/mnd2* animals (Fig. 4D). There is no accumulation of phosphorylated neurofilaments within cell bodies of *mnd2/mnd2* mice, in contrast to the accumulation observed in the mouse mutant wasted (*wst*) (Letsup and Rodriguez, 1989, and unpublished observations).

Nerve Conduction and Electromyography

Needle electromyography of hind limb muscles from affected *mnd2/mnd2* mice consistently revealed abnor-

mal spontaneous activity with fibrillation potentials and positive waves (Fig. 5). The severity of these changes correlated with advancing age. The pattern of spontaneous discharge in the mutant is characteristic of denervation.

Compound muscle action potential amplitudes in affected mice were 3.9 ± 1 mV ($n = 5$, mean \pm SEM), or less than half of the observed values in unaffected mice (13 ± 2 mV, $n = 4$; $P < 0.02$, unpaired two-tailed t test). This is indicative of a significant reduction in the number of motor axons innervating the muscle. Motor nerve conduction velocities did not differ in affected and unaffected mice [49 ± 1 m/s ($n = 4$) versus 52 ± 2 m/s ($n = 5$), respectively; $P > 0.15$], indicating that axon function is not qualitatively impaired in affected animals.

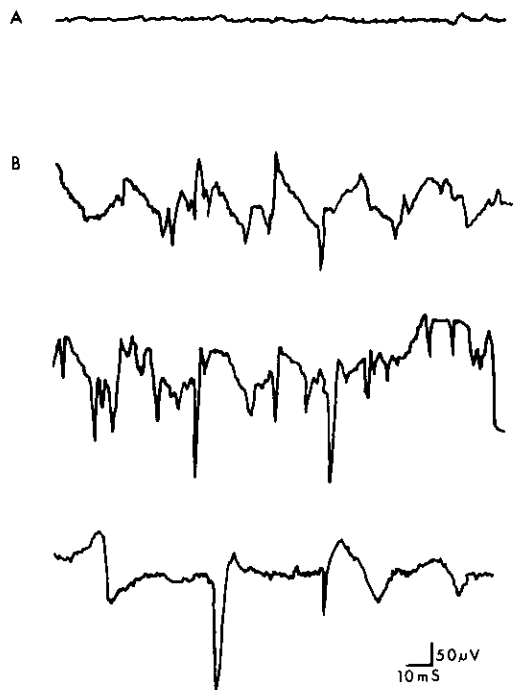


FIG. 5. Needle electromyography of sciatic-tibial innervated hind limb muscle. Abnormal spontaneous activity consisting of fibrillation potentials and positive waves is absent in an unaffected littermate (A) but visible in affected animals (B). Each trace was obtained from a different individual.

Regression of Lymphoid Organs

Spleen and thymus are normal in weight and appearance in 23-day-old animals at the time of onset of the disease. During disease progression, the size of both organs is reduced. At 34–40 days of age, in affected animals the wet weights of spleen (8.6 ± 2.3 mg, $n = 6$) and thymus (5.2 ± 1.1 mg, $n = 6$) are approximately 10% of the organ weights in unaffected littermates (78 ± 12 mg, $n = 5$ for spleen and 75 ± 19 mg, $n = 5$ for thymus). The histological appearance of the thymus is also normal at 23 days of age (Figs. 6A and 6B), but at 30 days there is dramatic regression of lymphoid cells, and the cortico-medullary junction is no longer visible (Fig. 6C). In spleen of affected animals there is atrophy of both lymphoid and hematopoietic tissue (not shown).

To determine whether the lymphoid deficiency was restricted to specific classes of cells, cell surface proteins and serum proteins were examined. Expression of several T cell and B cell surface antigens was analyzed by FACS analysis of cells from spleen and thymus, as described under Materials and Methods. Representative data are presented in Fig. 7. For all antigens examined, positive cells were present in normal frequencies in the affected animals both early and late in the disease, even though the total number of cells was greatly reduced at later stages. The proportions of serum immunoglobulins were also normal throughout the course of the disease. There is thus no evidence for loss of a specific lymphoid cell population.

Compound Heterozygotes with the Related Mutation, *wst*

The phenotype of *mnd2* mice is similar to the spontaneous *wasted* mutant with regard to time of onset, dis-

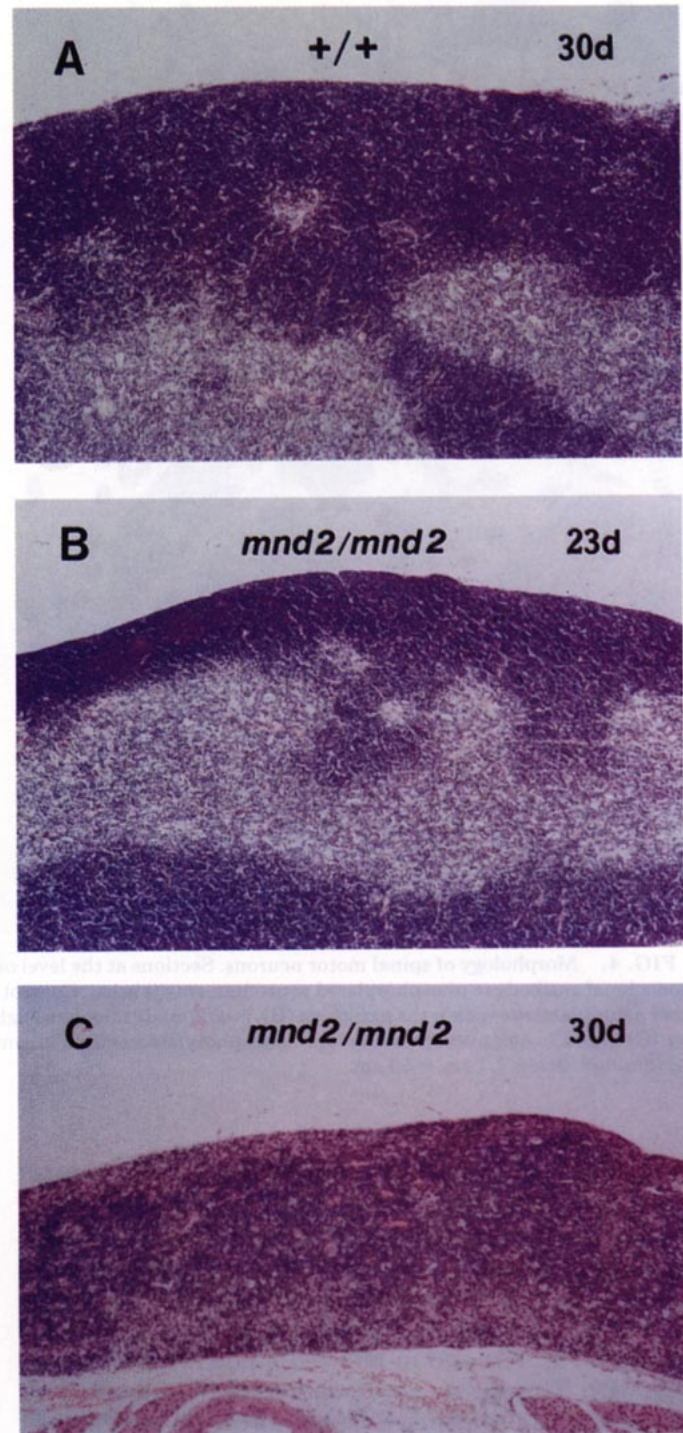


FIG. 6. Regression of the thymus in mutant mice. (A) Control with normal thymic architecture. (B) Affected animal at 23 days of age; the overall size of the organ and the distribution of cells between medulla and cortex are similar to control. (C) Affected animal at 30 days of age, with severe thymic atrophy and loss of the cortico-medullary junction. Sections were stained with eosin and hematoxylin. Magnification $\times 10$.

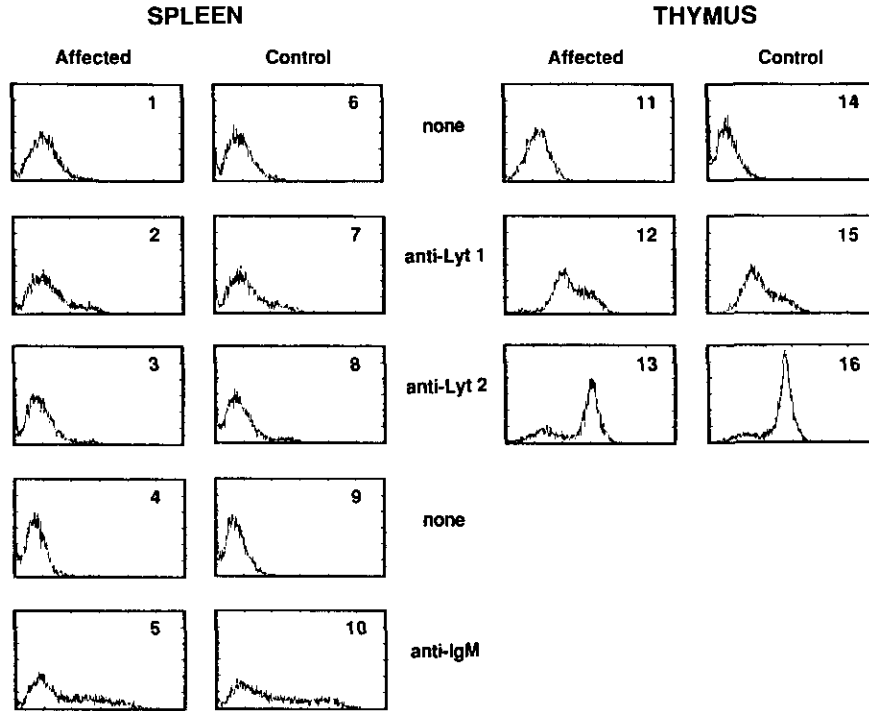


FIG. 7. Normal distribution of T and B cell antigens in spleen and thymus. Cells were prepared from affected *mnd2/mnd2* mice and littermate controls and analyzed at 30 days of age as described under Materials and Methods. Relative cell number is plotted on the ordinate and log fluorescent intensity on the abscissa. Background fluorescence with streptavidin-FITC in the absence of primary antibody (none) is compared with fluorescence in the presence of biotinylated anti-Lyt1 to stain helper T cells, anti-Lyt2 to stain cytotoxic T cells, and anti-IgM to stain most B cells. Panels 4, 5, 9, and 10 were obtained in a separate experiment from the other panels.

ease progression, regression of thymus and spleen, and involvement of anterior horn cells (Letsup and Rodriguez, 1989; Shultz *et al.*, 1982). We carried out a complementation test in which *mnd2/+* heterozygotes were crossed with *wst/+* heterozygotes. Among the 68 offspring of this cross, with the expectation of 17 compound heterozygotes, there were no animals with any characteristics of either mutant. Thus there is no double heterozygous effect of these two nonallelic mutations.

DISCUSSION

mnd2 produces an autosomal recessive disorder characterized by progressive paralysis and muscle atrophy. The abnormal morphology of spinal motor neurons and the muscle denervation in the absence of abnormal nerve conduction are indicative of a primary dysfunction in the growth or maintenance of motor neurons. The normal staining of myelinated fiber tracts indicates preservation of corticospinal fibers, and there was no obvious deficit in the number of pyramidal neurons in the motor cortex. The clinical course and histology most closely resemble human early onset spinal motor atrophy I or Werdnig-Hoffman syndrome (Brooke, 1986), except for the perikaryal accumulation of phosphorylated neurofilament, which has been described in some patients with spinal muscular atrophy (Lippa and

Smith, 1988; Kato and Hirano, 1990; Murayama *et al.*, 1991).

The time of onset and course of progression are quite reproducible in affected animals, with death between 35 and 40 days of age. We did not observe a significant effect of genetic background on the phenotype, even in crosses with the subspecies *Mus musculus castaneus*, which differs at many loci from the standard inbred strains. The early onset and reproducible time course will make this a good model for therapeutic trials, since prolongation of survival time would provide a readily quantifiable measure of improvement. Treatment with ciliary neurotrophic factor has recently been found to prevent neuronal degeneration in mice homozygous for the mutation *pmn* (progressive motor neuropathy) (Sendtner *et al.*, 1992). It will be valuable to extend this type of study to other mutants and growth factors to clarify the relationship between etiology and efficacy of treatment.

At least five mouse loci are associated with various types of motor neuron disease (Table 2). The spontaneous, semidominant mutation motor neuron degeneration (*Mnd*) produces degeneration of upper and lower motor neurons at 5 to 9 months, with neuronal inclusion bodies suggestive of a storage disease (Messer *et al.*, 1987, 1992). The wobbler mutation (*wr*) produces early onset and slow progression over a period of months, with degeneration of motor neurons in the spinal cord and

TABLE 2
Genes Responsible for Inherited Motor Neuron Disease in Human and Mouse

Gene symbol	Chromosomal location	Predicted homolog	Clinical phenotype	Reference
Mouse				
<i>Mnd</i>	Chr 8	Not known	Late, upper and lower	Messer <i>et al.</i> (1992)
<i>mnd2</i>	Chr 6	HSA 2p13	Early, lower	This paper
<i>pmn</i>	not known	Not known	Early, lower	Schmalbruch <i>et al.</i> (1991)
<i>tb</i>	Chr 1	HSA 2q3	Early	Green <i>et al.</i> (1989)
<i>wst</i>	Chr 2	HSA 20q	Early, lower	Shultz <i>et al.</i> (1982) Sweet <i>et al.</i> (1984)
<i>wr</i>	Chr 11	Not known	Late, upper and lower	Kaupmann <i>et al.</i> (1992)
Human				
<i>ALS1</i>	21q22	MMU 16	Late, upper and lower	Siddique <i>et al.</i> (1991)
<i>ALS2</i>	2q31-q35	MMU 1	Late, upper and lower	Hentati <i>et al.</i> (1992)
<i>SMA</i>	5q11-q13	MMU 13	Early and late, lower	Brzustowicz <i>et al.</i> (1990) Melki <i>et al.</i> (1990)

Note. The predicted locations of homologs are based on the location of the mapped gene within a conserved linkage group (Nadeau *et al.*, 1992). Clinical phenotype includes age of onset, with early and late corresponding to juvenile or adult onset; involvement of upper and/or lower motor neurons is indicated. HSA, *homo sapiens*; MMU, *Mus musculus*.

brainstem (Green, 1989). The wasted mutation (*wst*) affects lower motor neurons with early onset and rapid progression (Letsup and Rodriguez, 1989; Shultz *et al.*, 1982). The tumbler mutation (*tb*) produces early onset motor dysfunction with slow progression (Green, 1989). Progressive motor neuronopathy (*pmn*) produces an early onset and rapidly progressive disease similar in course to *mnd2*. To determine whether *pmn* might be allelic with *mnd2*, linkage of *pmn* with *D6Mit4* and *D6Mit6* has been tested; the observed nonlinkage indicates that the two mutations are not allelic (A. Brunialti and J.-L. Guenet, pers. comm., Jan. 1993).

Approximately 80% of human inherited motor neuron disease is due to mutation at the *SMA* locus on chromosome 5 (Table 2). Linkage to *SMA* has been observed in early and late onset families. Based on the location of markers closely linked to *SMA*, including hexosaminidase B, dihydrofolate reductase, and MAP1B, we predict that the mouse homolog would be located within a conserved linkage group on mouse chromosome 13 (Nadeau *et al.*, 1992). Similarly, the mouse homolog of the human *ALS1* locus is predicted to map to chromosome 16. A conserved linkage group on mouse chromosome 6 and human chromosome 2p12-p13 includes the genes *IgK*, *Cd8*, *Fabp1*, *Sftp3*, and *Tgfa* (Spurr and White, 1991; Nadeau *et al.*, 1992; D. C. Lee, pers. comm., Aug. and Dec. 1992). *mnd2* is located in the interval between *Sftp3* and *Tgfa* (unpublished observations). The mouse mutants in Table 2 are not likely to be homologs of *SMA* or *ALS1*, but they may be related to less common human mutations that have not yet been mapped. Since human *ALS2* and the mouse tumbler (*tb*) mutation are located within the same conserved linkage group (Nadeau *et al.*, 1992) they may represent homologs. Better characterization of the motor neuron pathology in the tumbler

mouse and comparison with the human disease would therefore be of great interest.

Although the underlying molecular defects in motor neuron disease have not yet been identified, neural growth factors and their receptors and downstream mediators may be considered likely candidates. Insulin like growth factor 1 and ciliary neurotrophic factor are known to prevent motor neuron death in cultured cells and in the *pmn* mutant *in vivo* (Sendtner *et al.*, 1992; Arakawa *et al.*, 1990; Oppenheim *et al.*, 1991). A defective growth factor that is required by both lymphoid cells and neurons could account for the regression of spleen and thymus that is also observed in *mnd2* mice. Regression of the lymphoid organs does not appear to be secondary to malnutrition, since it precedes the final, paralytic stage of the disease. The time of onset of symptoms in homozygous mice, close to the time of weaning, is consistent with the possibility that a missing factor is provided in the milk. In *Caenorhabditis elegans*, degeneration of specific neurons can result from mutations in genes encoding neuronal cell membrane proteins (Chalfie and Wolinsky, 1990; Driscoll and Chalfie, 1991). Related mammalian genes could be another source of motor neuron disease.

A high frequency of insertional mutations with biologically interesting phenotypes have been observed among transgenic mice (Meisler, 1992). Although there is no transgenic DNA linked with the *mnd2* locus, the origin of this mutation in a new transgenic line suggests that it is probably another example of an insertional mutation that was followed by deletion of the foreign DNA. The product of the *mnd2* gene appears to play a vital role in maintenance of motor neurons. Molecular cloning of *mnd2* will contribute to understanding the biology and pathogenesis of these cells. The early onset and consis-

tent disease course also make this mutant a useful model for evaluation of pharmacologic and genetic therapies.

ACKNOWLEDGMENTS

We thank Kevin Kaatz for excellent assistance with histology of the spinal cord, Dr. Marina Mata for performance of electron microscopic studies, Dr. Leonard Shultz for providing *wst/+* mice. We are grateful to Jeffrey Whitt and Jeffrey Friedman for providing probes. Supported by the Dr. Louis Sklarow Memorial Fund and the Muscular Dystrophy Association (M.H.M.), NS19613 and NS01300 (R.L.A.), NS01381 (E.L.F.), and CA33093 (B.A.T.).

REFERENCES

- Arakawa, Y., Sendtner, M., and Thoenen, H. (1990). Survival effects of ciliary neurotrophic factor (CNTF) on chick embryonic motoneurons in culture: Comparison with other neurotrophic factors and cytokines. *J. Neurosci.* **10**: 3507-3515.
- Bahary, N., Zorich, G., Pachter, J. E., Leibel, R. L., and Friedman, J. M. (1991). Molecular genetic linkage maps of mouse chromosomes 4 and 6. *Genomics* **11**: 33-47.
- Brooke, M. H. (1986). In "A Clinician's View of Neuromuscular Disease," 2nd ed., pp. 36-69, Williams & Wilkins, Baltimore, MD.
- Brzustowicz, L. M., Lehner, T., Castilla, L. H., Penchaszadeh, G. K., Wilhelmson, K. C., Daniels, R., Davies, K. E., Leppert, M., Ziter, F., Wood, D., Dubowitz, V., Zerres, K., Hausmanowa-Petrusewicz, I., Ott, J., Munsat, T. L., and Gilliam, T. C. (1990). Genetic mapping of chronic childhood-onset spinal muscular atrophy to chromosome 5q11.2-13.3. *Nature* **344**: 540-541.
- Chalfie, M., and Wolinsky, E. (1990). The identification and suppression of inherited neurodegeneration in *Caenorhabditis elegans*. *Nature* **345**: 410-416.
- Dietrich, W., Katz, H., Lincoln, S. E., Shin, H.-S., Friedman, J., Dracopoli, N. C., and Lander, E. S. (1992). A genetic map of the mouse suitable for typing intraspecific crosses. *Genetics* **131**: 423-447.
- Driscoll, M., and Chalfie, M. (1991). The *mec-4* gene is a member of a family of *Caenorhabditis elegans* genes that can mutate to induce neuronal degeneration. *Nature* **349**: 588-593.
- Elliott, R. W., and Moore, K. J. (1992). Mouse Chromosome 6. *Mamm. Genome* **3**: S81-S103.
- Green, M. C. (1989). Catalog of mutant genes and polymorphic loci. In "Genetic Variants and Strains of the Laboratory Mouse" (M. F. Lyon and A. G. Searle, Eds.), pp. 12-403, New York/Oxford UP.
- Hearne, C. M., McAleer, M. A., Love, J. M., Aitman, T. J., Cornall, R. J., Ghosh, S., Knoght, A., Prins, J.-B., and Todd, J. A. (1991). *Mamm. Genome* **1**: 273-282.
- Hentati, A., Bejaoui, K., Pericak-Vance, M. A., Hentati, F., Hung, W.-Y., Figlewicz, D. A., Ben Hamida, C., Ben Hamida, M., Brown, R. H., and Siddique, T. (1992). The gene locus for one form of juvenile amyotrophic lateral sclerosis maps to chromosome 2. *Neurology* **42**(Suppl): 201.
- Kaatz, K. W., Bazzett, T. J., and Albin, R. L. (1992). A new, simple myelin stain. *Brain Res. Bull.* **29**: 697-698.
- Kato, S., and Hirano, A. (1990). Ubiquitin and phosphorylated neurofilament epitopes in ballooned neurons of the extraocular muscle nuclei in a case of Werdnig-Hoffman disease. *Acta Neuropathol. (Berlin)* **80**: 334-337.
- Kaupmann, K., Simon-Chazottes, D., Guenet, J.-L., and Jockusch, H. (1992). Wobbler, a mutation affecting motoneuron survival and gonadal functions in the mouse, maps to proximal chromosome 11. *Genomics* **13**: 39-43.
- Keller, S. A., Rosenberg, M. P., Johnson, T. M., Howard, G., and Meisler, M. H. (1990). Regulation of amylase gene expression in diabetic mice is mediated by a *cis*-acting upstream element close to the pancreas-specific enhancer. *Genes & Dev.* **4**: 1316-1321.
- Kozak, C. A., Gunnell, M. A., and Rapp, U. R. (1984). A new oncogene, *c-raf*, is located on mouse Chromosome 6. *J. Virol.* **49**: 297-299.
- Letsup, H. L., and Rodriguez, M. (1989). Ultrastructural, morphometric and immunocytochemical study of anterior horn cells in mice with 'wasted' mutation. *J. Neuropathol. Exp. Neurol.* **48**: 519-533.
- Lippa, C. F., and Smith, T. W. (1988). Chromatolytic neurons in Werdnig-Hoffman disease contain phosphorylated neurofilaments. *Acta Neuropathol. (Berlin)* **77**: 91-94.
- McKeever, P. E., and Balentine, J. D. (1987). Nervous system. In "Histochemistry in Pathologic Diagnosis" (S. S. Spicer, Ed.), pp. 930-931, Dekker, New York.
- Meisler, M. H. (1992). Insertional mutation of 'classical' and novel genes in transgenic mice. *Trends Genet.* **8**: 341-344.
- Melki, J., Abdelhak, S., Sheth, P., Bachelot, M. F., Burlet, P., Marcadet, A., Aicardi, J., Barois, A., Carriere, J. P., Fardeau, M., Fontan, D., Ponsot, G., Ferriere, G., Lanzi, G., Ottolini, A., Babron, M. C., Cohen, D., Hanauer, A., Clerget-Darpoux, F., Lathrop, M., Munnich, A., Frezal, J. (1990). Gene for chronic proximal spinal muscular atrophies maps to chromosome 5q. *Nature* **344**: 767-768.
- Messer, A., Plummer, J., Maskin, P., Coffin, J. M., and Frankel, W. N. (1992). Mapping of the motor neuron degeneration (*Mnd*) gene, a mouse model of amyotrophic lateral sclerosis (ALS). *Genomics* **18**: 797-802.
- Messer, A., Strominger, N. L., and Mazurkiewicz, J. E. (1987). Histo-pathology of the late-onset motor neuron degeneration (*Mnd*) mutant in the mouse. *J. Neurogenet.* **4**: 201-213.
- Moore, K. J., D'Amore Bruno, M. A., Korfhagen, T. R., Glasser, S. W., Whitsett, J. A., Jenkins, N. A., and Copeland, N. G. (1992). Chromosomal localization of three pulmonary surfactant protein genes in the mouse. *Genomics* **12**: 388-393.
- Murayama, S., Bouldin, T. W., and Suzuki, K. (1991). Immunocytochemical and ultrastructural studies of Werdnig-Hoffman disease. *Acta Neuropathol. (Berlin)* **81**: 408-417.
- Nadeau, J. H., Davison, M. T., Doolittle, D. P., Grant, P., Hillyard, A. L., Kosowsky, M., and Roderick, T. H. (1992). Comparative map for mice and humans. *Mamm. Genome* **3**: 480-536.
- Oppenheim, R. W., Prevet, D., Quin-Wei, Y., Collins, F., and MacDonald, J. (1991). Control of embryonic motoneuron survival *in vivo* by ciliary neurotrophic factor. *Science* **251**: 1616-1618.
- Parry, G. J., and Kozu, H. (1990). Piroxicam may reduce the rate of progression of experimental diabetic neuropathy. *Neurology* **40**: 1446-1449.
- Schmalbruch, H., Skovgaard Jensen, H.-J., Bjoerg, M., Kamieniecka, Z., and Kurland, L. (1991). A new mouse mutant with progressive motor neuronopathy. *J. Neuropathol. Exp. Neurol.* **50**: 192-204.
- Sendtner, M., Schmalbruch, H., Stockli, K. A., Carroll, P., Kreutzberg, G. W., and Thoenen, H. (1992). Ciliary neurotrophic factor prevents degeneration of motor neurons in mouse mutant progressive motor neuronopathy. *Nature* **358**: 502-504.
- Shultz, L. D., Sweet, H. O., Davison, M. T., and Coman, D. R. (1982). 'Wasted,' a new mutant of the mouse with abnormalities characteristic of ataxia telangiectasia. *Nature* **297**: 402-404.
- Siddique, T., Figlewicz, D. A., Pericak-Vance, M. A., Haines, J. L., Rouleau, G., Jeffers, A. J., Sapp, P., Hung, W. Y., Behout, J., McKenna-Yasek, D., Deng, G., Horvitz, H. R., Gusella, J. F., Brown, R. H., and Roses, A. D. (1991). Linkage of a gene causing familial amyotrophic lateral sclerosis to chromosome 21 and evidence of genetic-locus heterogeneity. *N. Engl. J. Med.* **324**: 1381-1384.
- Spurr, N. K., and White, R. (1991). Report of the committee on the genetic constitution of chromosome 2. *Cytogenet. Cell Genet.* **58**: 142-169.
- Sternberger, L. A., and Sternberger, N. H. (1983). Monoclonal antibodies distinguish phosphorylated and nonphosphorylated forms of neurofilaments *in situ*. *Proc. Natl. Acad. Sci. USA* **80**: 6126-6130.
- Sweet, H. O. (1984). Wasted linkage. *Mouse News Lett.* **71**: 31.
- Taylor, B. A., and Rowe, L. (1989). A mouse linkage testing stock possessing multiple copies of the endogenous ecotropic mouse leukemia virus genome. *Genomics* **5**: 221-232.